

Measuring the Contrast Sensitivity Function Using the qCSF Method With 10 Digits

Haiyan Zheng¹, Chenxiao Wang¹, Rong Cui¹, Xianghang He¹, Menglu Shen¹, Luis Andres Lesmes², Zhong-Lin Lu³, Jia Qu¹, and Fang Hou¹

¹ School of Ophthalmology & Optometry and Eye Hospital, Wenzhou Medical University, Wenzhou, Zhejiang, China

² Adaptive Sensory Technology, Inc., San Diego, CA, USA

³ Center for Cognitive and Brain Sciences, Center for Cognitive and Behavioral Brain Imaging, and Department of Psychology, The Ohio State University, Columbus, OH, USA

Correspondence: Zhong-Lin Lu, The Ohio State University, Department of Psychology, 1835 Neil Ave, PS 62, Columbus, OH 43210, USA. e-mail: lu.535@osu.edu

Jia Qu, Wenzhou Medical University, School of Ophthalmology & Optometry and Eye Hospital, 270 Xue Yuan Xi Rd, Wenzhou, Zhejiang 325027, China. e-mail: jia.qu@163.com

Fang Hou, Wenzhou Medical University, School of Ophthalmology & Optometry and Eye Hospital, 270 Xue Yuan Xi Rd, 315 Teaching Building, Wenzhou, Zhejiang 325027, China. e-mail: houf@mail.eye.ac.cn

Received: 20 July 2018

Accepted: 28 September 2018

Published: 14 November 2018

Keywords: contrast sensitivity function; Bayesian adaptive procedure, qCSF; Sloan digit; precision

Citation: Zheng H, Wang C, Cui R, He X, Shen M, Lesmes LA, Lu Z-L, Qu J, Hou F. Measuring the contrast sensitivity function using the qCSF method with 10 digits. *Trans Vis Sci Tech.* 2018;7(6):9, <https://doi.org/10.1167/tvst.7.6.9>

Copyright 2018 The Authors

Purpose: The Bayesian adaptive quick contrast sensitivity function (qCSF) method with a 10-letter identification task provides an efficient CSF assessment. However, large populations are unfamiliar with letters and cannot benefit from this test. To overcome the barrier, we conducted this study.

Method: A new font for digits (0~9) was created. The digits were then filtered with a raised cosine filter, rescaled to different sizes to cover spatial frequencies from 0.5 to 16 cycles per degree (cpd), and used as stimuli in a 10-alternative forced choice (10AFC) digit identification task. With the 10AFC digit identification task, the CSFs of five young and five old observers were measured using the qCSF and Psi methods. The estimates from the latter served as reference.

Results: The new digit font showed significantly improved similarity structure, Levene's test, $F(1, 88) = 6.36, P = 0.014$. With the 10-digit identification task, the CSFs obtained with the qCSF method matched well with those obtained with the Psi method (root mean square error [RMSE] = 0.053 log₁₀ units). With approximately 30 trials, the precision of the qCSF method reached 0.1 log₁₀ units. With approximately 75 trials, the precision of the CSFs obtained with the qCSF was comparable to that of the CSFs measured by the Psi method in 150 trials.

Conclusions: The qCSF with the 10 digit identification task is validated for both young and old observers.

Translational Relevance: The qCSF method with the 10-digit identification task provides an efficient and precise CSF test especially for people who are unfamiliar with letters.

Introduction

The contrast sensitivity function (CSF) provides a comprehensive assessment of spatial vision at a variety of spatial frequencies,¹ and is used to evaluate and screen a variety of visual disorders.^{2–8} The

conventional CSF measurement in the laboratory is very time-consuming,⁹ while the clinically available chart for CSF assessment, such as the Vistech chart or Functional Acuity Contrast Test (FACT) exhibited very poor test–retest reliability.^{10,11} Recently, Lesmes et al.¹² developed the Bayesian adaptive quick CSF

(qCSF) method to efficiently measure the CSF with high precision and accuracy. The method was further improved by incorporating a 10-alternative forced choice (10AFC) letter identification task.¹³

In addition to its efficiency and precision, the qCSF has shown great test–retest reliability as well as sensitivity in detecting changes of visual functions.¹⁴ The qCSF has been used to measure the CSF in several clinical populations, including subjects with amblyopia,^{15,16} multiple sclerosis,⁶ dry age-related macular degeneration,¹⁷ central serous chorioretinopathy (Marmalidou, et al. *IOVS*, 2018;59:ARVO E-Abstract 3126), glaucoma,¹⁸ early diabetic retinopathy,¹⁹ and aging.²⁰ It also has been used to investigate dynamic effects of visual adaptation,²¹ the time course of postoperative recovery of the CSF of patients who experienced extended periods of early-onset blindness,²² visual performance change after blur adaptation,²³ and the impact of emotional arousal on the CSF,²⁴ as well as CSF in peripheral vision.²⁵ These studies demonstrated the potential of the qCSF method in clinical applications.

The qCSF method implemented with the 10AFC task and Sloan letter stimuli is approximately two times more efficient than that implemented with the 2AFC grating orientation identification task in the original qCSF development.¹³ Letter identification is also a task more relevant to daily vision than the grating orientation identification task.²⁶ However, people in non-Latin alphabet–using countries who are unfamiliar with English letters cannot benefit from the more efficient qCSF test with letter stimuli. To address this problem, we implemented the qCSF method with a new set of Arabic digit stimuli in a 10AFC digit identification task in this study.

The Arabic numeral set, 0–9, is the most commonly used symbolic system in the world.²⁷ Arabic digit stimuli already have been used in assessing visual acuity (Early Treatment of Diabetic Retinopathy Study [ETDRS] number charts; Precision Vision, Woodstock, IL), contrast sensitivity,²⁸ and crowding effects.²⁹ However, the digit fonts used to generate the stimuli in those studies are not suitable for the CSF test. The fonts used in the ETDRS number chart and contrast sensitivity chart of Khambhaphanta et al.²⁸ are very similar. Both have a very uneven similarity structure in which digits 3, 6, 8, and 9 are much more confusable with each other than with the other digits. Khambhaphanta et al.²⁸ found that their observers performed much worse in identifying digits 3, 6, 8, and 9 than other digits. This is probably why only a subset of the 10 digits is used in the ETDRS number

chart and the Khambhaphanta et al.²⁸ contrast sensitivity chart. Since test efficiency increases with the number of alternatives in forced-choice identification tasks,¹³ using only a subset of the 10 digits would make the test less efficient. It also may introduce unwanted memory burdens on the observer³⁰ and additional complications to the underlying psychophysical model of the qCSF test.

The crowding chart designed by Pelli et al.²⁹ has nine digits with a font specially designed to have a 1:5 width-to-height ratio to measure crowding effects. The 1:5 width-to-height ratio renders the digits not suitable for the CSF test because they became very difficult to recognize after we filtered them with a radially isotropic log-cosine filter.^{31,32} Here, we redesigned the font of the digit stimuli for the qCSF test.

In this study, we aim to implement and validate the qCSF method in a 10AFC task with a new digit optotype set. We first redesigned the font of the 10 digits so that the digit stimuli had a more even similarity structure among them and, thus, less response bias. The digits were bandpass filtered to create suitable stimuli for the CSF test. The similarity structure of digit stimuli in the new font were examined and compared with that of digit stimuli used by Khambhaphanta et al.²⁸ We then implemented the qCSF method with the new digit stimuli and validated the method with young and old observers. The latter are representative of a Chinese population that cannot read letters. For the purpose of validation, the Psi method³³ was used to provide an independent measure of contrast sensitivity in a range of spatial frequencies. The results obtained from the Psi method were used as references to evaluate qCSF performance. Because CSF has been reported to decrease with age,³⁴ we also evaluated the performance of the qCSF method in detecting the CSF difference between the old and young observers.

Methods

Observers

Five graduate students (25.8 ± 1.10 years) at Wenzhou Medical University and five old observers (65.0 ± 5.15 years) from the local communities in Wenzhou, Zhejiang, China participated in the study. All but one author (Y5) were naive to the study purpose. All observers had normal or corrected-to-normal vision (minimal angle resolvable [MAR], ≤ 1.0 arcmin) and no history of mental diseases. The young

observers showed no sign of any eye disease. The old observers showed no sign of eye disease other than cataract. They were free from diabetes, hypertension, and cognitive deficits (Mini-Mental State Examination [MMSE] > 26 points). An ophthalmologist (author #2) and a graduate student in ophthalmology and optometry (author #1) prescribed the best optical corrections at the test distance for all observers. The study protocol adhered to the tenets of the Declaration of Helsinki and was approved by the institutional review board of human subjects' research of the Eye Hospital, Wenzhou Medical University. Written informed consent was obtained from each observer before the experiment.

Apparatus

The programs used in the experiment were written in MATLAB (MathWorks, Natick, MA) with Psychtoolbox extensions³⁵ and run on a Mac minicomputer (Model No. A1347; Apple, Inc., Cupertino, CA). Stimuli were displayed on a gamma-corrected Asus flat panel monitor (PG279Q; Asus Corp., Taipei, Taiwan) with a mean luminance of 91.2 cd/m². The display had a spatial resolution of 2560 × 1440 pixels and a refresh rate of 60 Hz. Each pixel subtended 0.01° at a viewing distance of 1.34 m. A bit-stealing algorithm was used to achieve 9-bit gray-scale resolution.³⁶ Observers viewed the display binocularly with their best corrections, if any, in a dark room. A chin/forehead rest was used to minimize head movement during the experiment.

Stimuli

The new digit font was designed to follow the specifications for Sloan optotypes.³⁷ The detailed specifications for the new digit font are shown in Figure 1a. To improve the similarity structure among the digit stimuli, major changes were made to digits 3, 6, and 9 to reduce the similarities among them.

All 10 digits in the new font were filtered with a raised cosine filter that had a center frequency of 3 cycles per object and a full bandwidth at half height of 1 octave.^{31,32} The pixel intensity of each filtered image was normalized by the maximum absolute intensity of the image such that, after normalization, the maximum absolute Michelson contrast of the image is 1.0 (Fig. 1b). Stimuli with different contrasts were obtained by scaling the intensities of the normalized images with corresponding contrast values. The filtered images were resized to generate stimuli with different central spatial frequencies (Fig. 1c).

Design

The CSF was measured with the qCSF method.^{12,13} In addition, contrast sensitivities at 0.50, 1, 2, 4, 8, and 15.8 cycles per degree (cpd) were measured using the Psi method.³³ Each observer finished four experimental sessions in four separate days. One experimental session comprised 300 trials of two consecutive qCSF runs (150 trials × 2 runs) randomly interleaved with 300 trials of the Psi method to measure contrast sensitivities at six spatial frequencies (50 trials × 6 frequency conditions), and lasted approximately 50 minutes.

In the beginning of the experiment, observers were given approximately 200 practice trials to become familiar with the experimental setting and procedure. Before starting each day's session, observers were given 5 minutes to adapt to the dark test environment. Some old observers who usually did not wear spectacles were given an additional 25 minutes to become used to their prescribed optical correction.

Procedure

Each trial began with a brief tone signaling its onset and the presentation of a crosshair fixation (250 ms) in the center of the screen, followed by a blank screen (125 ms) with background luminance (91.2 cd/m²). Then, a filtered digit stimulus was presented for 133 ms, followed by a 500 ms response screen that showed all 10 digits to facilitate response collection. The stimulus duration of 133 ms was used because it was short enough to minimize potential effects of saccade³⁸ and also long enough to reach the critical stimulus duration for temporal integration at the spatial frequencies tested.^{39,40}

Digits in the response screen were arranged as a 2 × 5 matrix and presented in the center of the display. Same paradigm was used in our previous work.³² Young observers were instructed to use the keyboard to type or mouse to select the digit they saw. Old observers were asked to verbally report the identity of the test digit. Their responses were entered by the experimenter via the computer keyboard. No feedback was provided during the experiment. A new trial started 500 ms after the response.

Analysis

To examine the properties of the new digit stimuli, the complex wavelet structural similarity indexes (CW-SSIM)⁴¹ were calculated for the 10 digits in our newly created font. The CW-SSIM is an image similarity index based on textural and structural properties of localized regions of an image pair. It

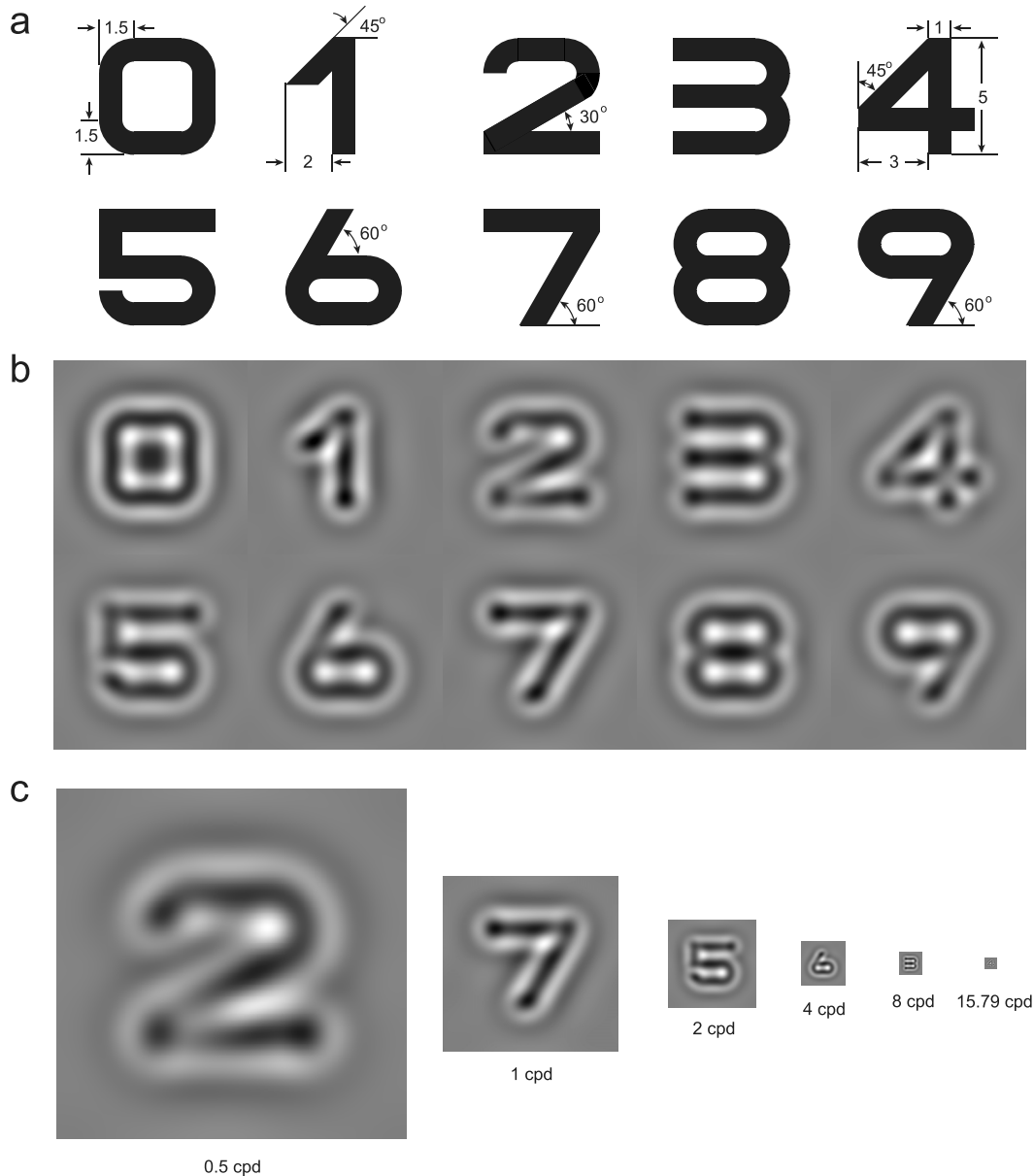


Figure 1. (a) The new digit font shown with design specifications. (b) Band-pass filtered digit stimuli. (c) Filtered digit stimuli in different spatial frequency conditions.

takes into account the properties of the human visual system and is insensitive to small rotations and translations. For the 10-digit images, the CW-SSIM matrix is 10×10 , with ones on the main diagonal (the similarity of two identical images is one). Because the CW-SSIM matrix is symmetric (the similarity between images A and B is the same as that between images B and A), we only analyzed the 45 pairwise CW-SSIMs between different digits. The same procedure was followed to obtain the CW-SSIMs of the 10 digits created by Khambhiphanta et al.²⁸ and the filtered

images of the new digits. Comparisons of the two CW-SSIM matrices were made.

As a parametric procedure, the qCSF method estimates the entire CSF curve represented by the four parameters: peak gain, peak spatial frequency, bandwidth at half-height, and low-frequency truncation level.^{12,42} The contrast sensitivities at desired spatial frequencies, the area under the log CSF curve (AULCSF), which is a widely used summary metric of the CSF function,^{15,43,44} and the cutoff spatial frequency (Cut-Off), which characterizes the high-

frequency resolution of the visual system^{45,46} can be derived from the measurement.

To directly compare the results from the qCSF and Psi methods, contrast sensitivities at 0.50, 1, 2, 4, 8, and 15.8 cpd were derived from the qCSF measurement and used in the analysis. Unless otherwise stated, the average CSFs of the observers across all measurement sessions were used in comparing the two methods and in evaluating the difference between the two groups.

In computing the correlation coefficient between the estimated CSFs from the two methods, calculation of precision and RMSE of the estimated CSFs from the qCSF method, and determining the sensitivity of the qCSF method in detecting the CSF difference between the young and old groups, the CSF from a single qCSF run or the CSFs of all eight runs were used.

Results

Properties of the New Digit Font

The CW-SSIMs of the 10 digits in the new font are plotted against those in the font used by Khambhiphanta et al.²⁸ in Figure 2. The mean CW-SSIMs for the digits in the font used by Khambhiphanta et al.²⁸ and the new font were 0.373 ± 0.240 and 0.355 ± 0.166 , respectively. Histograms of the CW-SSIMs of the digits in the two fonts also are shown on the top and left of Figure 2, respectively. The variability of the CW-SSIMs of the digits with the new font is significantly less than that of the digits with the font used in the Khambhiphanta et al.²⁸ chart, Levene's test, $F(1, 88) = 6.36$, $P = 0.014$. This result suggested that the similarity structure of the digit has been significantly improved in the new font.

Because filtered digits were used to measure CSF, we also computed the CW-SSIM of the filtered digits in the new font. Filtering greatly reduced the variability of the similarity between digit pairs. The mean CW-SSIM was 0.608 ± 0.126 for the filtered digit stimuli. The variance of the CW-SSIM of the filtered digit stimuli was marginally smaller than that for the unfiltered digits, Levene's test, $F(1, 88) = 3.02$, $P = 0.086$. The coefficient of variation (relative standard deviation) of the CW-SSIM for the filtered digit stimuli 20.7% was quite small.

Comparing CSFs Measured by the qCSF and Psi Methods

Figure 3 shows the estimated CSFs from the qCSF method (red curves) and the estimated contrast

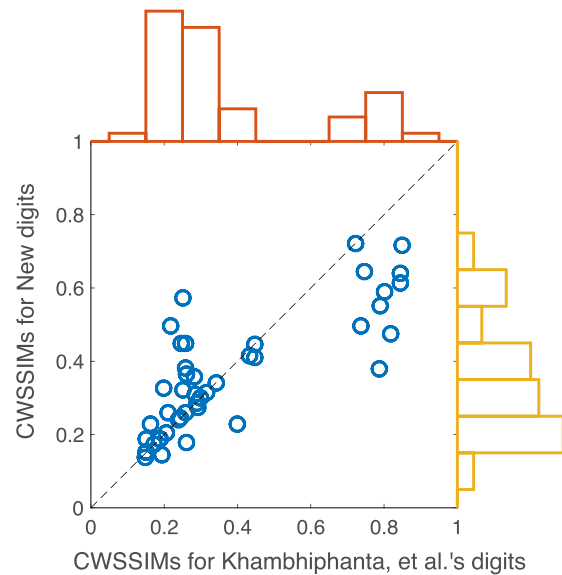


Figure 2. The CW-SSIMs of the digits in the new font are plotted against those of the digits in the font used by Kambhiphanta et al.²⁸ The histogram on the top of the figure shows the distribution of the CW-SSIM of the digit stimuli in the font of Kambhiphanta et al.²⁸ The histogram on the left shows the distribution of CW-SSIM of the digit stimuli in the new font.

sensitivities at the six spatial frequencies from the Psi method (blue circles) for each observer. The estimated contrast sensitivities from the two methods matched well with each other, indicating good validity of the qCSF test.

Using the estimated contrast sensitivities from the Psi method as references, we could quantitatively check the validity of the qCSF method. With the truncated parabola assumption, the contrast sensitivities obtained from the qCSF method were constrained by the functional form across spatial frequencies. We could not directly compute the correlation coefficient between the estimated contrast sensitivities obtained by the qCSF and Psi methods. Here, we used a novel procedure developed previously¹⁴ to assess the correlation between the estimated CSFs from the two methods. The general idea is to eliminate the constraints on the estimated contrast sensitivities obtained from the qCSF method by using estimated contrast sensitivity at each spatial frequency from different qCSF measurements. (1) For each of the six spatial frequencies, we randomly selected one of the eight qCSF runs (without replacement) and obtained contrast sensitivities at that spatial frequency from the selected qCSF measurement; (2) we repeated step 1 six times to obtain contrast sensitivities at all six spatial frequencies, each of which was

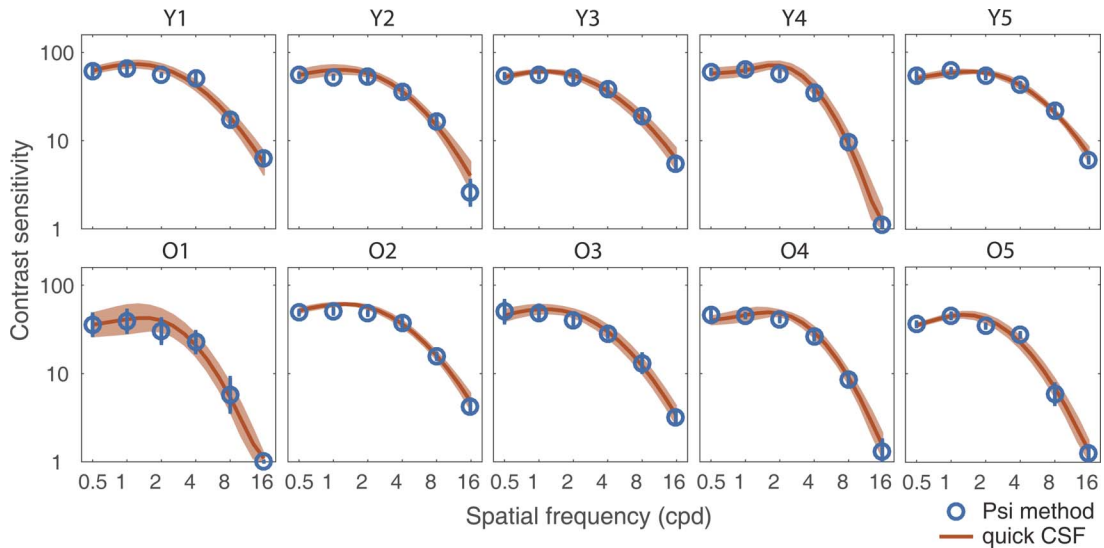


Figure 3. Estimated CSFs obtained with the qCSF method (red curves) and the Psi method (blue circles). Y1~Y5, young observers; O1 ~ O5, old observers. The red-shaded regions and the blue error bars indicate ± 1 inter-run SD for the qCSF and Psi methods, respectively.

from an independent qCSF run; (3) we performed steps 1 and 2 for all the observers; (4) we computed the correlation coefficient between the synthesized CSF and the CSF obtained from the Psi method across all spatial frequencies and observers; and (5) we repeated steps 1 to 4 five hundred times, and calculated the average correlation coefficient. The results of a single iteration (steps 1–4) of the procedure are shown in Figures 4a and 4b for the young and old observers, respectively.

In this procedure, the contrast sensitivities at different spatial frequencies are from completely different qCSF runs and, therefore, independent. The average correlation coefficient was $0.982 \pm$

0.005 and 0.985 ± 0.004 for the young and old observers, respectively, indicating that the estimated CSFs obtained with the qCSF method matched well with those obtained with the Psi method.

In addition to the correlation analysis, we performed a Bland-Altman analysis⁴⁷ to quantify the agreement between the estimated CSFs from the qCSF and Psi methods. Figures 5a and 5b show the Bland-Altman plots for the young and old observers. The mean difference was 0.017 and 0.023 log₁₀ units, respectively. In comparison, the limits of agreement were ± 0.126 and ± 0.120 log₁₀ units for the two groups, respectively.

We also computed the root mean squared error

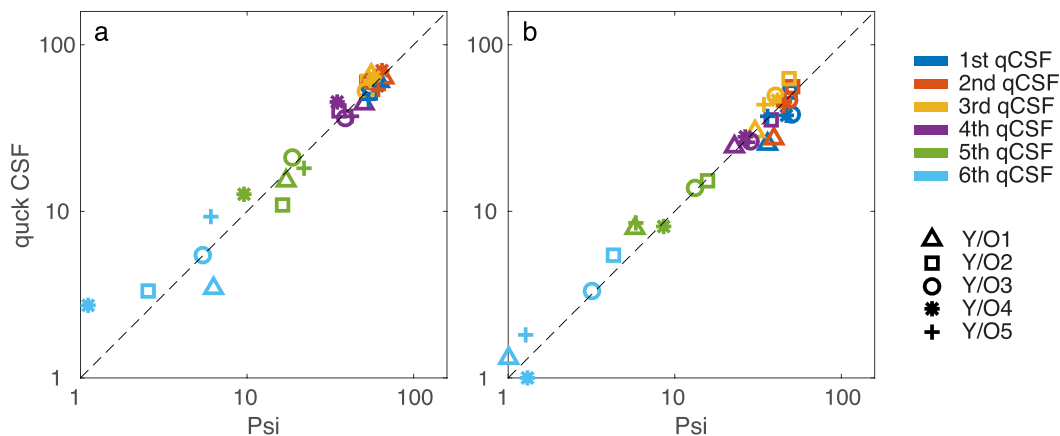


Figure 4. Illustration of a single iteration of the correlation analysis. The synthesized CSF consisted of six contrast sensitivities (each from a different qCSF run) plotted against the contrast sensitivities from the Psi method for the young (a) and old (b) groups. Different colors represent data obtained in different sessions. Different symbols represent data from different observers.

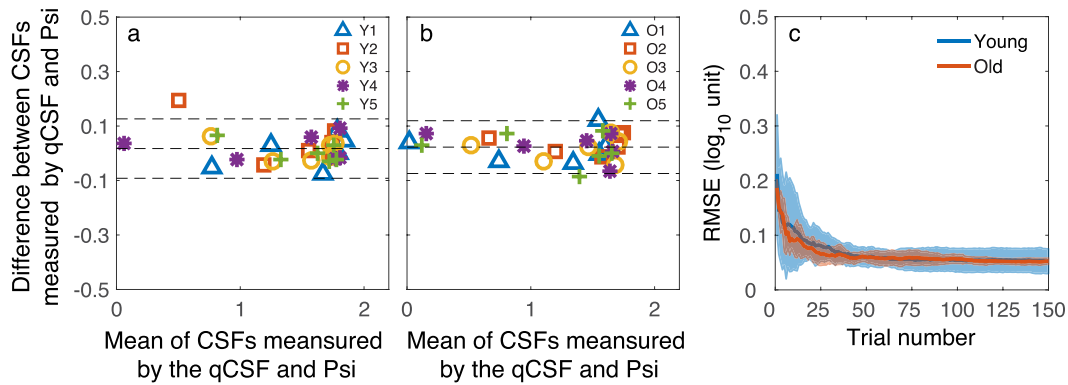


Figure 5. (a) The Bland–Altman plot of the estimated contrast sensitivities from the qCSF and Psi methods of the young group: the difference between the estimates from the two methods against the mean of the estimates from the two methods. (b) The Bland–Altman plot for the old group. Different symbols represent different observers. (c) The average RMSE of the young observers (blue curve) and old observers (red curve) as a function of qCSF trial number. Shaded area represents ± 1 SD.

(RMSE) between the estimated contrast sensitivities from each qCSF trial and the final estimates from the Psi method.⁴⁸ The RMSEs of the young and old observers are plotted as a function of trial number in Figure 5c. The RMSE decreased rapidly in the first 30 trials and leveled off to 0.053 ± 0.023 and 0.053 ± 0.006 log₁₀ units for the young and old observers, respectively. There was no significant difference between the RMSEs of the two groups, two-sample *t*-test, $t(8) = 0.011$, $P = 0.992$. Again, the estimated contrast sensitivities from the two methods matched well with each other.

Precision of the qCSF Method

The precision of a method is the reciprocal of the variability of its estimates. To examine the precision

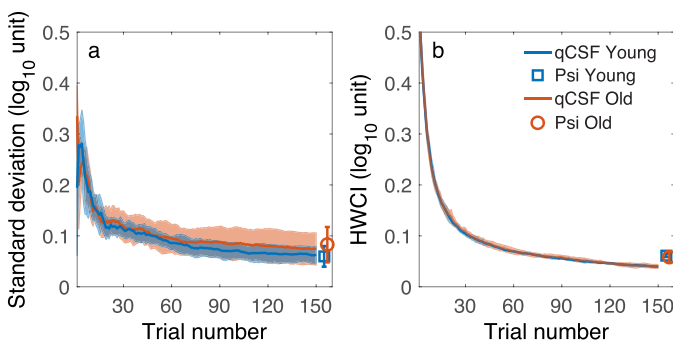


Figure 6. (a) The average standard deviations of the estimated CSFs from the qCSF method as functions of trial number for the two groups, along with the average SD from 150 Psi trials. (b) The average 68.2% HWCI of the estimated CSFs as functions of trial number for the two groups, along with the average HWCI from 150 Psi trials. Blue and red curves represent the results for the young and old groups, respectively. Shaded area represents ± 1 SD for the qCSF. Error bar: represents ± 1 SD for the Psi method.

of the qCSF method, we computed the standard deviation of the estimated CSFs from different qCSF runs and the half width of the 68.2% credible interval (HWCI)⁴⁹ of the posterior distribution of the CSF measured in a single run.^{13,14}

The average standard deviations (SD) of the estimated CSFs of the young and old observers are plotted as a function of trial number in Figure 6a. For both groups, the average SD decreased rapidly to 0.1 log₁₀ units in the first 30 trials, one-sample *t*-test, $t(4) = 1.83$, $P = 0.140$ for young observers; $t(4) = 1.40$, $P = 0.233$ for old observers, and leveled off to 0.063 ± 0.017 and 0.074 ± 0.032 log₁₀ units after approximately 60 trials for the young and old groups, respectively, with no significant difference in the asymptotic level between the groups, two-sample *t*-test, $t(8) = 0.693$, $P = 0.508$. For the young group, the average SD of the estimated CSFs from the qCSF method after 75 trials reached that of the estimated CSFs from the psi method in 150 trials, 0.076 ± 0.019 versus 0.060 ± 0.020 , paired *t*-test, $t(4) = 2.61$, $P = 0.06$. For the old group, the average SD of the estimated CSFs from the qCSF method after 60 trials reached that of the estimated CSFs from the psi method in 150 trials, 0.095 ± 0.027 versus 0.083 ± 0.035 , paired *t*-test, $t(4) = 2.05$, $P = 0.11$. The results suggested that the qCSF is much more efficient than the Psi method in estimating the CSF.

The average 68.2% HWCI of the estimated CSFs obtained with the qCSF method is plotted as functions of trial number in Figure 6b. Similar to the SD, the HWCI decreased rapidly in the first 30 trials, reached 0.1 log₁₀ units after 31 trials, one-sample *t*-test, $t(4) = 0.320$, $P = 0.765$ for young observers; $t(4) = 1.93$, $P = 0.126$ for old observers, and

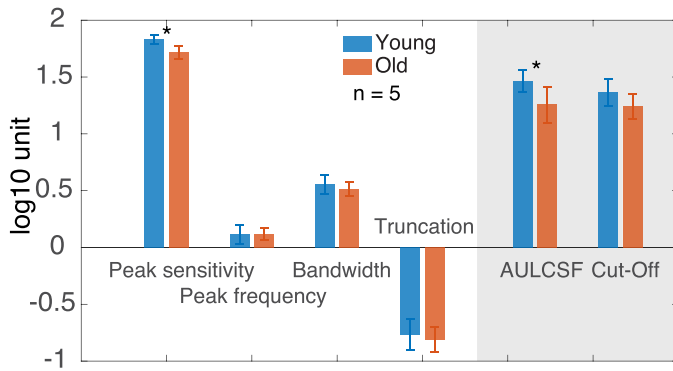


Figure 7. Group comparisons of CSF parameters. *Blue*, young group; *Red*, old group. Error bar: represents SD. *Statistical significance.

leveled off to 0.040 ± 0.002 and 0.040 ± 0.003 log₁₀ units after approximately 60 trials for the young and old groups, respectively, with no significant difference in the asymptotic level between the groups, two-sample *t*-test, $t(8) = 0.06$, $P = 0.954$. For the young group, the average HWCI of the estimated CSFs from the qCSF method after 75 trials reached that of the estimated CSFs from the Psi method in 150 trials, 0.065 ± 0.004 versus 0.062 ± 0.003 log₁₀ units, paired *t*-test, $t(4) = 2.06$, $P = 0.11$. For the old group, the average HWCI of the estimated CSFs from the qCSF method after 60 trials reached that of the estimated CSFs from the Psi method in 150 trials, 0.07 ± 0.007 versus 0.06 ± 0.01 log₁₀ units, paired *t*-test, $t(4) = 2.59$, $P = 0.061$. Again, the results suggest that the qCSF is approximately two times as efficient as the Psi method in estimating the CSF.

Comparing the CSFs Between the Young and Old Groups

For the estimated CSFs from the Psi method, a repeated measures analysis of variance (ANOVA) showed that group had a significant effect, $F(1, 8) = 7.7$, $P = 0.024$. There was a marginally significant interaction between group and spatial frequency, $F(1, 8) = 5.26$, $P = 0.051$. We also performed group comparisons on the CSF parameters obtained from the qCSF method, which included the peak sensitivity, peak frequency, bandwidth, truncation, AULCSF and the cutoff frequency^{12,15} (Fig. 7). The peak gain and AULCSF of the old group were significantly lower than those of the young group, two-sample *t*-test, $t(8) = 3.64$, $P = 0.007$ for peak sensitivity; $t(8) = 2.52$, $P = 0.036$ for AULCSF. No significant difference was found on peak frequency, cutoff frequency, bandwidth, and truncation (all P s > 0.05).

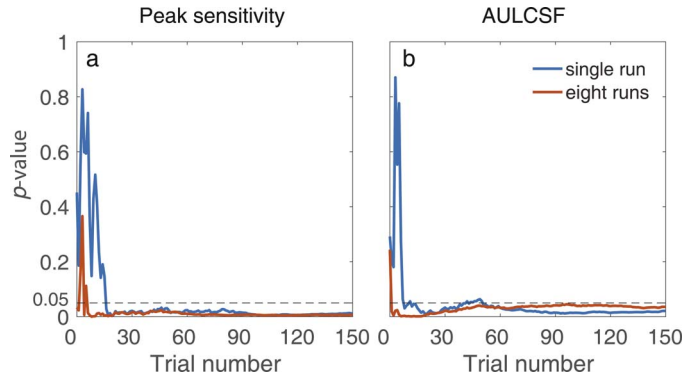


Figure 8. *P* values for group comparisons of peak sensitivity (a) and AULCSF (b) as functions of trial number. The *blue* curves represent *P* values for the two-sample *t*-test on the data from the first qCSF run. The *red* curves represent *P* values of the group effect in the repeated measure ANOVA on the data from all eight qCSF runs.

To evaluate the sensitivity of the qCSF in detecting the CSF difference between the young and old groups, we compared the peak sensitivity and AULCSF measured by the qCSF between the two groups in each trial. We ran two-sample *t*-tests on peak sensitivity and AULCSF measured in the first qCSF run. The *P* values for the comparisons are plotted as functions of trial number in Figures 8a and 8b, respectively. After 17 trials, the peak sensitivity difference between the two groups became significant, $t(8) = 2.67$, $P = 0.028$ in the 17th trial, and remained significant thereafter. After eight trials, the AULCSF difference between the two groups became significant, $t(8) = 2.60$, $P = 0.031$ at the eighth trial, and remained significant for most of the trial thereafter. We also ran a two-way repeated measure ANOVA on all eight qCSF runs. Trial number and group were within-subject and between-subject factors, respectively. The *P* values of the group effect are plotted as functions of trial number for peak sensitivity and AULCSF in Figures 8a and 8b. After only seven trials for peak sensitivity and one trial for AULCSF, the group effect became significant, peak sensitivity: $F(1, 8) = 9.92$, $P = 0.014$ in the 7th trial; AULCSF: $F(1, 8) = 9.10$, $P = 0.017$ in the 1st trial.

Discussion

In this study, our major aim was to implement the qCSF method in a 10-digit identification task for people who are not familiar with English letters. We first designed a new digit font, and then implemented

and validated the qCSF method with the 10-digit identification task with young and old observers. We found that the new digit font had a significantly improved similarity structure. The estimated CSFs from the qCSF method matched those measured by the Psi method (correlation coefficient > 0.98 , RMSE = $0.053 \log_{10}$ units). The standard deviation and 68.2% HWCI of the estimated CSFs from the qCSF method reached $0.1 \log_{10}$ units with approximately 30 trials or 3 minutes. The precision of the qCSF method with approximately 75 trials reached that of the Psi method in 150 trials. We also found that the qCSF can reveal the CSF difference between the young and old groups with fewer than 20 trials. The qCSF with 10-digit identification exhibited similar performance as the qCSF method with 10-AFC letter identification.¹³ Both qCSF methods can reach $0.1 \log_{10}$ units precision in 2 to 3 minutes.

For multialternative forced choice tasks (m-AFC), there could be response bias if all alternatives are nonorthogonal and nonequivalent.^{50,51} Based on signal detection theory,⁵² the response choices depend on the relative similarities among the alternative set. It has been found that the confusion matrix in letter recognition was determined by the similarity in spatial frequency content of the letters.⁵³ For digit stimuli with uneven similarities, some alternatives are more favored than others. In reality, we cannot completely eliminate the similarity between the digits. So the key of a good font design for the 10-digit identification task is to make the similarity of all digit pairs as equal as possible, that is, minimize the variance of the similarities across digit pairs. Our newly designed fonts for 10 digits had an improved similarity structure with reduced standard deviation of the similarity across digit pairs when compared to those used in the Khambhiphanta et al.²⁸ chart (SD of CW-SSIM, 0.166 vs. 0.234). Due to this improved similarity structure, we suggested that the digit font designed in the current study should be adopted by other visual tests with digit stimuli, such as visual acuity and contrast sensitivity charts.

For the CSF test, we filtered all the digit stimuli with a one-octave bandwidth log-cosine filter^{31,32} and reduced the difference in spatial frequency content among them. Although the mean CW-SSIM of the filtered digits was greater than that of the unfiltered digits (0.608 vs. 0.355, Wilcoxon signed rank test, $z = 5.84$, $P = 5.18 \times 10^{-9}$), the variability of the CW-SSIM of the filtered digits was only marginally smaller than that of the unfiltered digits, Levene's test, $F(1, 88) =$

3.02 , $P = 0.086$. Again, because the response choices depend on the relative not absolute similarities of the stimuli, the filtered stimuli should reduce the response bias during the CSF test.

As a Bayesian adaptive procedure, the qCSF method generates not only the estimated contrast sensitivity but also the variability of the contrast sensitivity in a single run. The intra-run variability of the estimated CSF, represented by the 68.2% HWCI of the posterior distribution of the CSF ($0.040 \log_{10}$ units), was less than the inter-run variability, represented by the standard deviation of repeated CSF estimates (0.063 ± 0.017 and $0.074 \pm 0.032 \log_{10}$ units for the young and old groups, respectively, Fig. 6), while our previous study reported that the HWCI and standard deviation were very similar.¹³ The observed difference in this study was probably due to a practice effect, which increased the intersession (across day) variability.

The qCSF method exploits a well-established functional relationship between contrast sensitivity and spatial frequency.⁴² Instead of measuring contrast sensitivity at one spatial frequency at a time, the qCSF method uses the information from the observer's response in every single trial at different spatial frequency and contrast condition to infer the entire CSF. The inference is based on two assumptions: (1) the CSF can be well described by a truncated log parabolic function with four parameters: peak gain, peak spatial frequency, bandwidth at half-height, and low-frequency truncation level; and (2) the slopes of psychometric functions at different spatial frequencies are the same. Violations of these assumptions can adversely affect the validity of the qCSF method, especially for clinical populations with significantly different optical and neural characteristics.³⁴ The first assumption was supported by the following results in the current study: (1) the correlation coefficient between the estimated CSFs from the qCSF and Psi methods was greater than 0.98, (2) the mean difference between the estimated contrast sensitivities from the two methods in the Bland-Altman analysis was 0.017 and $0.023 \log_{10}$ units for the young and old observers, respectively, and (3) the RMSE difference between the two methods, estimated across the tested frequencies, was $0.053 \log_{10}$ units. The second assumption was supported by the results in a parallel study, in which we collected data with a large number of trials for each digit stimulus in each spatial frequency condition (Zheng et al. Comparing contrast sensitivity functions measured using digit and grating stimuli.

In preparation). We investigated the psychometric properties of each individual digit and found that the slope of the psychometric function for all digits in all the spatial frequency conditions is essentially the same. Taken together, these results provide strong support of the underlying assumptions of the qCSF method in the 10AFC digit identification task.

The RMSE, standard deviation and HWCI of the estimated CSFs from the qCSF method were not significantly different between the young and old groups. The result suggested that the qCSF method with the 10 digit identification task is equally applicable for the young and old populations with normal sights. It is also consistent with the results from several previous qCSF studies that showed that the precision of the method did not depend on patients' overall level of visual deficits (Lesmes L, et al. *IOVS*. 2012;53:ARVO E-Abstract 4358; Rosen R, et al. *IOVS*. 2015;56:ARVO E-Abstract 2224; Ramulu PY, et al. *IOVS*. 2015;56:ARVO E-Abstract 2225; Babakhan L, et al. *IOVS*. 2015;56:ARVO E-Abstract 3901).^{15,54}

Although their visual acuities were normal, we found that the old observers had reduced CSF compared to the young observers, consistent with other studies in the literature.⁵⁵⁻⁵⁷ The AULCSF of the old group decreased by 0.21 log10 units compare to that of the young group. The magnitude of the AULCSF drop was less than the 0.31 log10 unit reported by Owsley et al.⁵⁸ One contributing factor is that our old observers had better visual acuity than those reported by Owsley et al.⁵⁸ (MAR 1.0 vs. 1.27). Another factor could be that the stimuli used for CSF testing in the two studies are different. We used digit stimulus and varied stimulus size at difference spatial frequencies while Owsley et al.⁵⁸ used grating stimulus with fixed stimulus size at all spatial frequencies. Consistent with our previous study,¹⁴ the qCSF method is very sensitive in detecting CSF changes between groups. With the 0.21 log10 unit AULCSF difference, we could detect the difference between the young and old groups in eight trials in a single run of the qCSF method or with one trial in each of eight qCSF runs.

Taken together, the qCSF method implemented in a 10AFC digit identification task delivers an accurate, precise, and efficient assessment of contrast sensitivity for both young and old non-Latin alphabet-using observers. In complement to our previous study of the qCSF method,^{13-15,20} our current results suggested that the qCSF method is a potentially powerful tool in clinical applications.

Acknowledgments

Supported by the National Natural Science Foundation of China (NSFC81600764 to FH), the National Key R&D Program of China (2016YFB0401203 to FH), Wenzhou Medical University (QTJ16006 to FH), and the National Eye Institute (EY021553 to ZLL).

Disclosure: **H. Zheng**, None; **C. Wang**, None; **R. Cui**, None; **X. He**, None; **M. Shen**, None; **L.A. Lesmes**, qCSF technology (P), Adaptive Sensory Technology, Inc. (I, E); **Z.-L. Lu**, qCSF technology (P), Adaptive Sensory Technology, Inc. (I); **J. Qu**, None; **F. Hou**, None

References

1. Ginsburg AP. Contrast sensitivity and functional vision. *Int Ophthalmol Clin*. 2003;43:5-15.
2. Hess RF, Howell ER. The threshold contrast sensitivity function in strabismic amblyopia: evidence for a two type classification. *Vision Res*. 1977;17:1049-1055.
3. Ginsburg AP. Contrast sensitivity: determining the visual quality and function of cataract, intraocular lenses and refractive surgery. *Curr Opin Ophthalmol*. 2006;17:19-26.
4. Kara S, Gencer B, Ersan I, et al. Repeatability of contrast sensitivity testing in patients with age-related macular degeneration, glaucoma, and cataract. *Arq Bras Oftalmol*. 2016;79:323-327.
5. Owidzka M, Wilczynski M, Omulecki W. Evaluation of contrast sensitivity measurements after retrobulbar optic neuritis in Multiple Sclerosis. *Graefes Arch Clin Exp Ophthalmol*. 2014;252:673-677.
6. Stellmann JP, Young KL, Pottgen J, Dorr M, Heesen C. Introducing a new method to assess vision: computer-adaptive contrast-sensitivity testing predicts visual functioning better than charts in multiple sclerosis patients. *Mult Scler J Exp Trans Clin*. 2015;1:2055217315596184.
7. Stavrou EP, Wood JM. Letter contrast sensitivity changes in early diabetic retinopathy. *Clin Exp Optom*. 2003;86:152-156.
8. Huang C, Tao L, Zhou Y, Lu ZL. Treated amblyopes remain deficient in spatial vision: a contrast sensitivity and external noise study. *Vision Res*. 2007;47:22-34.

9. Kelly DH, Savoie RE. A study of sine-wave contrast sensitivity by two psychophysical methods. *Percept Psychophys*. 1973;14:313–318.
10. Pesudovs K, Hazel CA, Doran RML, Elliott DB. The usefulness of Vistech and FACT contrast sensitivity charts for cataract and refractive surgery outcomes research. *Br J Ophthalmol*. 2004;88:11.
11. Elliott DB, Bullimore MA. Assessing the reliability, discriminative ability, and validity of disability glare tests. *Invest Ophthalmol Vis Sci*. 1993;34:108–119.
12. Lesmes LA, Lu ZL, Baek J, Albright TD. Bayesian adaptive estimation of the contrast sensitivity function: the quick CSF method. *J Vis*. 2010;10:1711–21.
13. Hou F, Lesmes L, Bex P, Dorr M, Lu ZL. Using 10AFC to further improve the efficiency of the quick CSF method. *J Vis*. 2015;15.
14. Hou F, Lesmes LA, Kim W, et al. Evaluating the performance of the quick CSF method in detecting contrast sensitivity function changes. *J Vis*. 2016;16:18.
15. Hou F, Huang CB, Lesmes L, et al. qCSF in clinical application: efficient characterization and classification of contrast sensitivity functions in amblyopia. *Invest Ophthalmol Vis Sci*. 2010;51:5365–5377.
16. Jia W, Zhou J, Lu ZL, Lesmes LA, Huang CB. Discriminating anisometric amblyopia from myopia based on interocular inhibition. *Vision Res*. 2015;114:135–141.
17. Lesmes LA, Jackson ML, Bex P. Visual function endpoints to enable dry AMD clinical trials. *Drug Discov Today*. 2013;10:e43–e50.
18. Lin S, Mihailovic A, West SK, et al. Predicting Visual Disability in Glaucoma With Combinations of Vision Measures. *Transl Vis Sci Technol*. 2018;7:22–22.
19. Joltikov KA, de Castro VM, Davila JR, et al. Multidimensional functional and structural evaluation reveals neuroretinal impairment in early diabetic retinopathy. *Invest Ophthalmol Vis Sci*. 2017;58:BIO277–BIO290.
20. Yan F-F, Hou F, Lu Z-L, Hu X, Huang C-B. Efficient characterization and classification of contrast sensitivity functions in aging. *Sci Rep*. 2017;7:5045.
21. Gepshtein S, Lesmes LA, Albright TD. Sensory adaptation as optimal resource allocation. *Proc Natl Acad Sci U S A*. 2013;110:4368–4373.
22. Kalia A, Lesmes LA, Dorr M, et al. Development of pattern vision following early and extended blindness. *Proc Natl Acad Sci U S A*. 2014;111:2035–2039.
23. Venkataraman AP, Winter S, Unsbo P, Lundström L. Blur adaptation: contrast sensitivity changes and stimulus extent. *Vision Res*. 2015;110:100–106.
24. Lee TH, Baek J, Lu ZL, Mather M. How arousal modulates the visual contrast sensitivity function. *Emotion*. 2014;14:978–984.
25. Rosen R, Lundstrom L, Venkataraman AP, Winter S, Unsbo P. Quick contrast sensitivity measurements in the periphery. *J Vis*. 2014;14:3.
26. Pelli DG, Robson J, Wilkins A. The design of a new letter chart for measuring contrast sensitivity. *Clin Vision Sci*. 1988;2:187–199.
27. Bulliet R, Crossley P, Headrick D, Hirsch S, Johnson L. *The Earth and Its Peoples: A Global History*, 5th ed. Boston, MA: Cengage Learning; 2010:512.
28. Khambhiphanta B, Tulvatanab W, Busayarath M. The new numbers contrast sensitivity chart for contrast sensitivity measurement. *J Optom*. 2011;4:128–133.
29. Pelli DG, Waugh SJ, Martelli M, et al. A clinical test for visual crowding [version 1; referees: 2 approved with reservations]. *F1000Research* 2016;5:81.
30. Jakel F, Wichmann FA. Spatial four-alternative forced-choice method is the preferred psychophysical method for naive observers. *J Vis*. 2006;6:1307–1322.
31. Chung ST, Legge GE, Tjan BS. Spatial-frequency characteristics of letter identification in central and peripheral vision. *Vision Res*. 2002;42:2137–2152.
32. Hou F, Lu ZL, Huang CB. The external noise normalized gain profile of spatial vision. *J Vis*. 2014;14:9.
33. Kontsevich LL, Tyler CW. Bayesian adaptive estimation of psychometric slope and threshold. *Vision Res*. 1999;39:2729–2737.
34. Owsley C. Aging and vision. *Vision Res*. 2011;51:1610–1622.
35. Kleiner M, Brainard D, Pelli D. What's new in Psychtoolbox-3? *Perception*. 2007;36:14–14.
36. Tyler CW. Colour bit-stealing to enhance the luminance resolution of digital displays on a single pixel basis. *Spatial Vis*. 1997;10:369–377.
37. Committee on Vision NRC, National Academy of Sciences, Washington, D.C. Recommended Standard Procedures for the Clinical Measurement and Specification of Visual Acuity. *Adv Ophthalmol*. 1980;41:103–148.
38. Purves D, Augustine GJ, Fitzpatrick D, et al. *Neuroscience*. Sunderland, MA: Sinauer Associates; 2001.

39. Breitmeyer BG, Ganz L. Temporal studies with flashed gratings: inferences about human transient and sustained channels. *Vision Res.* 1977;17: 861–865.
40. Legge GE. Sustained and transient mechanisms in human vision: temporal and spatial properties. *Vision Res.* 1978;18:69–81.
41. Sampat MP, Wang Z, Gupta S, Bovik AC, Markey MK. Complex wavelet structural similarity: a new image similarity index. *IEEE Trans Image Proc.* 2009;18:2385–2401.
42. Watson AB, Ahumada AJ. A standard model for foveal detection of spatial contrast. *J Vis.* 2005;5: 717–740.
43. Applegate RA, Howland HC, Sharp RP, Cottingham AJ, Yee RW. Corneal aberrations and visual performance after radial keratotomy. *J Refract Surg.* 1998;14:397–407.
44. Oshika T, Okamoto C, Samejima T, Tokunaga T, Miyata K. Contrast sensitivity function and ocular higher-order wavefront aberrations in normal human eyes. *Ophthalmology.* 2006;113: 1807–1812.
45. Zhang X, An X, Liu H, et al. The topographical arrangement of cutoff spatial frequencies across lower and upper visual fields in mouse V1. *Sci Rep.* 2015;5:7734.
46. Regan D, Beverley KI. Visual fields described by contrast sensitivity, by acuity, and by relative sensitivity to different orientations. *Invest Ophthalmol Vis Sci.* 1983;24:754–759.
47. Giavarina D. Understanding Bland Altman analysis. *Biochem Med.* 2015;25:141–151.
48. Kim W, Pitt MA, Lu ZL, Steyvers M, Myung JI. A hierarchical adaptive approach to optimal experimental design. *Neural Comput.* 2014;26: 2465–2492.
49. Clayton D, Hills M. *Statistical Models in Epidemiology.* Oxford, UK: Oxford University Press; 1993.
50. Hacker MJ, Ratcliff R. A revised table of d' for M-alternative forced choice. *Percept Psychophys.* 1979;26:168–170.
51. Klein SA. Measuring, estimating, and understanding the psychometric function: a commentary. *Percept Psychophys.* 2001;63:1421–1455.
52. DeCarlo LT. On a signal detection approach to m-alternative forced choice with bias, with maximum likelihood and Bayesian approaches to estimation. *J Math Psychol.* 2012;56:196–207.
53. Gervais MJ, Harvey LO, Roberts JO. Identification confusions among letters of the alphabet. *J Exp Psychol Hum Percept Perform.* 1984;10:655–666.
54. Lesmes L, Wallis J, Jackson ML, Bex P. The reliability of the quick CSF method for contrast sensitivity assessment in low vision. *Invest Ophthalmol Vis Sci.* 2013;54:2762.
55. Crassini B, Brown B, Bowman K. Age-related changes in contrast sensitivity in central and peripheral retina. *Perception.* 1988;17:315–332.
56. Elliott D, Whitaker D, MacVeigh D. Neural contribution to spatiotemporal contrast sensitivity decline in healthy ageing eyes. *Vision Res.* 1990;30:541–547.
57. Burton KB, Owsley C, Sloane ME. Aging and neural spatial contrast sensitivity: photopic vision. *Vision Res.* 1993;33:939–946.
58. Owsley C, Sekuler R, Siemsen D. Contrast sensitivity throughout adulthood. *Vision Res.* 1983;23:689–699.